Mechanism Behind the Dependence of Thrust on Facility Backpressure and Implications on the Operation of the SPT-140 Onboard the Psyche Mission

IEPC-2019-410

Ioannis G. Mikellides*, Alejandro Lopez Ortega†, Vernon H. Chaplin‡, John Steven Snyder§
Jet Propulsion Laboratory, California Institute of Technology, Pasadena, CA, 91109

Giovanni Lenguito**
Maxar, Palo Alto, CA, 94303

Presented at the 36th International Electric Propulsion Conference
University of Vienna • Vienna, Austria
September 15-20, 2019

Abstract

The Psyche mission will employ Stationary Plasma Thrusters (SPT-140) for primary propulsion in space and will be the first to use Hall thrusters beyond lunar orbit. One of the longest standing risks in the implementation of this EP technology on missions like Psyche is our limited understanding of the effects of ground test facilities on the performance and wear of the thruster. It has been well-known for example that thrust increases as the facility backpressure is raised, sometimes by as much as ~10% in Hall thrusters with external cathodes. Since the true conditions in space cannot be reproduced in ground tests even in our best vacuum facilities, such changes in thrust yield large uncertainties in performance predictions during spaceflight. An analytical model of the thrust has been developed to provide insight into Hall thruster performance dependence on facility pressure. Inputs to the model have been provided by 2-D (r-z) axisymmetric simulations with the Hall2De code. The combined analyses yields very good agreement with thrust measurements from ground tests of the SPT-140 and suggests two new findings. First, at intermediate pressures the rise of the thrust with increasing pressure is mainly due to fast atoms produced by charge exchange collisions with beam ions. The location of the acceleration region remains unchanged and the thrust rise is linear with pressure. As the pressure increases further, displacements of the acceleration region become non-negligible and reduce the rate of increase in thrust. Second, the thrust rise at low pressures is

*Principal Engineer, Electric Propulsion Group, 4800 Oak Grove Drive, Pasadena, CA, 91109, Mail Stop 125-109.
†Member of the Technical Staff, Electric Propulsion Group, 4800 Oak Grove Drive, Pasadena, CA, 91109, Mail Stop 125-109.
‡Member of the Technical Staff, Electric Propulsion Group, 4800 Oak Grove Drive, Pasadena, CA, 91109, Mail Stop 125-109.
§Senior Engineer, Electric Propulsion Group, 4800 Oak Grove Drive, Pasadena, CA, 91109, Mail Stop 125-109.
**Propulsion Development Engineer, Propulsion Group, 3825 Fabian Way, Palo Alto, CA, 94303.

driven largely by transport of electrons *along* magnetic lines, from the cathode to the near-plume of the thruster, which explains why it is non-linear with pressure. It is argued based on first-principles that this higher rate of thrust variation observed at the lowest pressures may be strongly linked to the highly asymmetric distribution of the external-cathode electrons around the discharge. These findings suggest that thrust in space may be predicted by a combination of modeling and ground measurements that take into account variations of pertinent plasma properties in the azimuthal direction.

Nomenclature

$\mathbf{F}$ = propulsive force, N
ρ = mass density of heavy species, kg/m^3
$\mathbf{u}$ = velocity of heavy species, m/s
u_{i_z} = z-component of the ion velocity, m/s
u_{ib} = ion velocity at location "b", m/s
$C_{i\text{-}n}$ = relative velocity during ion-atom charge-exchange collision, m/s
A = thrust integration area, m^2
$\hat{n}$ = unit vecto
T = total thrust, N
T_i = thrust from ions, N
T_n = thrust from atoms, N
m = mass of the heavy species, kg
n_i = total number density of ions, m^{-3}
n_n = total number density of atoms, m^{-3}
n_e = total number density of electrons, m^{-3}
$\tilde{n}_e$ = azimuthally-averaged total number density of electrons, m^{-3}
$\dot{n}_{cex}$ = production rate of fast atoms from charge-exchange collisions with ions, m^{-3}s^{-1}
V = thrust integration volume, m^3
$c_{cex1,2}$ = constants in energy fit to the change-exchange collision cross section area, σ, m^2
$c_{n_{1,2}}$ = integration constants associated with the contribution of atoms to the total thrust
k = Boltzmann's constant, 1.381×10^{-23} J/K
n^F_{nref} = reference number density of Facility (F) atoms, m^{-3}
p_F = facility pressure (Torr Xe)

<u>Greek Symbols</u>

β = dimensionless pressure scaling factor
$\Theta_{i/n}$ = ion/atom temperature, K
θ = ion divergence angle (rad)
ℓ_{cex} = characteristic length within which change- exchange collisions occur, m
σ =cross section area of charge-exchange collisions, m^2
ϕ = plasma potential, V
Θ_e = electron temperature, eV
ν_α = anomalous collision frequency, s^{-1}

<u>Subscripts</u>

A At the Anode (A) location
B At the intersection of the reference B-line (B) and the channel centerline
C At the exit of the keeper orifice, on the Cathode (C) centerline

q	= ion charge, C		b	At location "b" of the ion beam, the intersection between the thrust integration path and the channel centerline
r	= radial distance from thruster centerline, m			
r_{ref}	= reference radial distance from thruster centerline, m			Superscripts
f_i	= function determining the variation of the Thruster (T) ion number density along a radial thrust integration path		T	Contribution to particle number densities by the Thruster
f_n	= function determining the variation of the Thruster (T) atom number density along a radial thrust integration path		C	Contribution to particle number densities by the Cathode
c_i	= integration constant associated with the contribution of thruster ions (ion beam) to the total thrust		F	Contribution to particle number densities by the Facility

I. INTRODUCTION

NASA's Psyche mission is planned for launch in 2022 on a journey to the largest metal asteroid in the solar system [1]. The mission will be enabled by Stationary Plasma Thrusters (SPT-140) and will be the first to use Hall thrusters beyond lunar orbit [2]. It will also carry the most xenon ever flown on a single NASA spacecraft. In ground tests at the NASA Glenn Research Center (GRC) performance measurements of the SPT-140 over the power range 0.9-4.5 kW produced the now well-observed variations of thrust with facility pressure. The tests showed that the largest change occurred at the 4.5-kW operation during which the thrust increased by about 7.2% from 3.2 μTorr to 34.2 μTorr. Such variation was notably larger than the experimental uncertainty in the measurements [3]. Thrust dependence on pressure declined with power until there was little-to-no measurable effect at 0.9 kW.

Changes in the performance of Hall thrusters when the ground facility pressure is varied is a well-observed phenomenon that occurs most prominently when they are operated with externally-mounted cathodes. Most investigations to better understand this phenomenon have been experimental and aimed largely at providing empirical trends of thruster performance [3-7] and/or plasma measurements [7-10] with varying backpressure. More recently, such investigations have been extended to include facility electrical effects [11, 12]. Of particular interest in this article is the well-known increase of the thrust with increasing facility pressure. To this end, though several conjectures have been made over the years based largely on the abovementioned experimental investigations, the understanding of what drives this dependence remained too elusive to allow physics-based predictions of thruster performance in space. This remains true today despite the significant advancements that 2-D numerical simulations have achieved over the last two decades.

The increased risk associated with the uncertainty in the physics that drive the performance dependence on facility pressure, naturally, affects adversely the performance and lifetime margins for science missions employing this type of Solar Electric Propulsion (SEP) technology, like Psyche. During the SPT-140 ground tests at NASA GRC, a critical finding at the higher power conditions was that the thrust variation at the lowest pressures was non-linear and displayed no asymptotic trend. The implication for Psyche is that the true thrust in (space) vacuum could not be predicted with high certainty by these measurements alone. This prompted a focused modeling and simulation effort to elucidate the observed trends and is the subject of this and our companion [13] articles.

In [13] we report on the findings of numerical simulations with the 2-D axisymmetric code Hall2De [14] that aimed to, first, validate the simulations using measurements from the performance tests at NASA GRC and, second, provide estimates of thruster life for the Psyche mission profile. In this article we expand on the insights gained from that work by combining the simulation results with a new analytical model for the thrust. Unlike previous semi-empirical and phenomenological thrust models, (e.g. see [15] and references therein), the model developed here is expressed directly in terms of the fundamental properties of the plasma, paying close attention to the thrust contribution by the non-ionized background gas. The impetus behind this approach is our direct access to the extensive range of plasma properties available in the numerical simulations, an advantage that is not offered by plasma diagnostics alone. Our expectation has been that such access would allow us to interrogate the various contributions to the thrust at a level of detail not achievable by phenomenological thrust models or measurements, and in less time than that required to execute several numerical simulations. The article is structured as follows. Section II provides the pertinent background on the SPT140 measurement and Hall2De simulations. The theoretical model for the thrust is developed in Sec. III. Results from the model and comparisons with both the simulations and the measurements are discussed in Sec. IV. The article concludes with Sec. V.

II. PERFORMANCE MEASUREMENTS AND 2-D (r-z) NUMERICAL SIMULATIONS

The SPT-140 is produced by Fakel EDB (Kaliningrad, Russia) and consists mainly of an annular anode, a discharge channel, an external cathode and an internal magnetic circuit containing electromagnet coils and a pole structure [16]. The propellant is injected homogeneously from a stainless steel ring at the base of the discharge channel which also serves as the anode electrode. The cathode contains a lanthanum hexaboride (LaB_6) thermionic emitter and is located externally as shown in Fig 1. Though two cathodes are shown only one is used during thruster operation. The second cathode is redundant.

In a recent effort to characterize the performance of the SPT-140 as a function of background pressure, p_F, over the power range planned for the Psyche mission, a series of tests were conducted at NASA GRC. The measurements reported in this article were performed in GRC's Vacuum Facility 5 (VF-5). Information pertinent to the chamber, pumping system and operation, facility pressure measurements and the electrical configuration of the thruster can be found in [3] and references therein. The thrust stand was of the inverted pendulum style, which upon calibration yielded uncertainty in the thrust measurements of ±2.1 mN to ±2.6 mN. Thrust measurements as a function of p_F were obtained for operating conditions ranging 3-15 A of discharge current and 0.9-4.5 kW of discharge power. The discharge voltage was 300 V for all conditions. Thrust dependence on pressure declined with power until there was little-to-no measurable effect at 0.9 kW. A comparison of the normalized values at 2.5 and 4.6 kW is shown in Fig 2-top. In this paper we focus only on the 4.5 kW (15 A) condition since it exhibited the largest variation in thrust for the range of pressures the facility was operated. Referring to Fig 2-bottom, at the lowest value (p_F=3.2 μTorr) the measured thrust was as low as 278.7 mN and at the highest value (p_F=34.2

μTorr) it was 298.7 mN. This constitutes an increase of 20 mN (7.2%) over a ~10× increase in p_F, and is a larger change than the ~3% observed in tests of the SPT-100 over approximately the same p_F range [4]. The error bars in Fig 2-bottom represent fixed uncertainties of ±2.5 mN for thrust and ±7% for p_F. It is worth noting that the thrust rate of change was highest at the lowest pressures and exhibited no signs of an asymptotic trend. The implication for Psyche is that the true thrust in (space) vacuum could not be predicted with high certainty by these measurements alone.

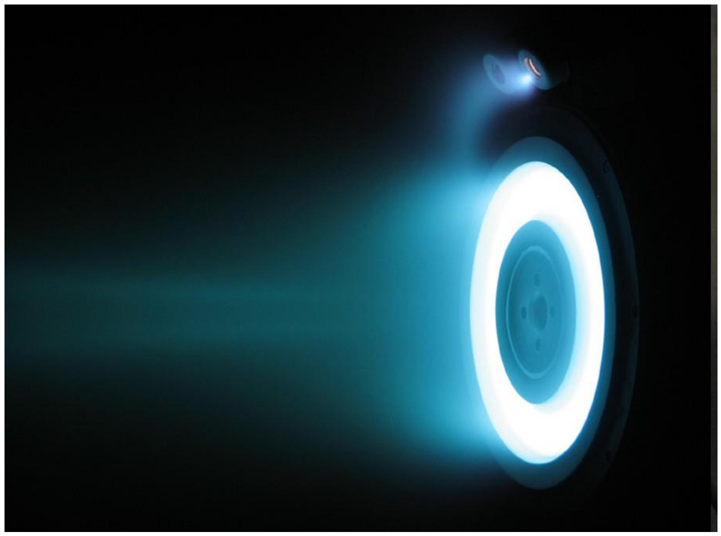

Fig 1. The SPT-140 operating in a ground facility showing two external cathodes only one of which is used.

The findings from the ground tests prompted a focused modeling and simulation effort to elucidate the observed trends. Numerical simulations of the SPT-140 were performed with the two-dimensional (2-D), axisymmetric code Hall2De [14] and are described in detail in our companion paper [13]. The governing equations, computational methods, and simulations of several other thrusters have been reported in several other articles [14, 17-19]. Therefore we provide here only a brief overview of the code for completeness.

The Hall2De governing equations are discretized on a computational mesh that is aligned with the applied magnetic field to reduce the numerical diffusion associated with the large plasma anisotropy of the plasma in these devices. The magnetic-field-aligned-mesh (MFAM) spans a computational domain in r-z geometry that is large enough to encompass the cathode boundary. The conservation equations are based largely on the formulations of Braginskii for a partially ionized gas [20]. In Hall2De we compute the neutral gas density using line-of-sight formulations that account for ionization [21]. The ions are divided into multiple isothermal fluids and each fluid is associated with a distinct energy bin [14, 22]. Typically, a Hall2De simulations will account separately for at least the main-beam ions and "slow" ions associated with the cathode. In the SPT-140 simulations three fluid energy bins were specified that accounted for singly-, doubly- and triply-charged ions in each fluid.

The electron population in Hall2De is also treated as a fluid. The generalized Ohm's law is solved in two directions on the MFAM and the electrical resistivity accounts for classical momentum-transfer electron collisions with ions and neutrals. It is now also widely accepted (but poorly understood) that the diffusion of electron mass and heat in Hall thrusters is enhanced “anomalously” by plasma turbulence (e.g. see [23-27]). In numerical simulations this enhancement has typically been modeled using an effective or “anomalous” collision frequency we shall denote ν_α. The approach to define ν_α in Hall2De yields a near-continuous function is described in detail in [28]. The most accurate Hall thruster simulations are achieved when ion velocity measurements obtained by (non-intrusive) methods such as Laser Induced Fluorescence (LIF) are used to guide ν_α, which is what was done in the present investigation.

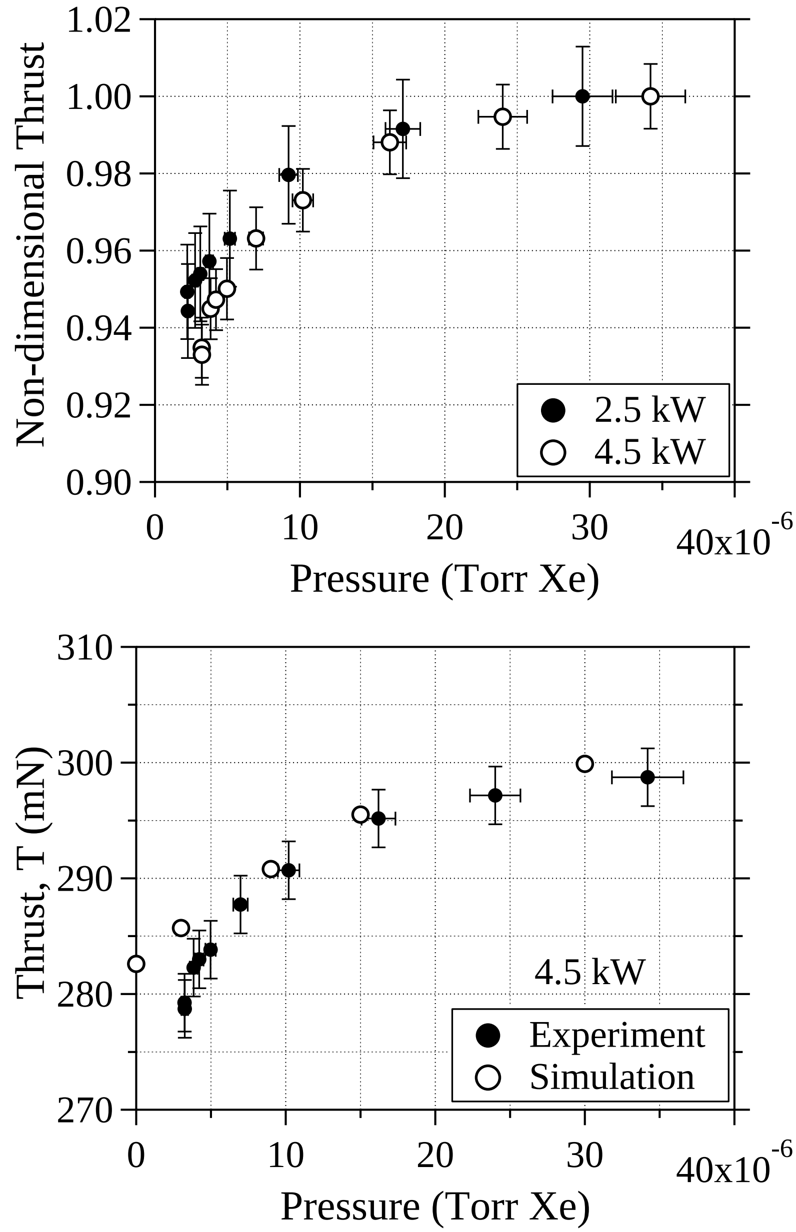

Fig 2. Thrust as a function of facility pressure. Top: Comparison of normalized values at 2.5 and 4.5 kW. Bottom: Comparison between Hall2De simulations and measurements. Negligible movement of the acceleration zone was detected by LIF measurements when the pressure was lowered from 15 to 9 μTorr. No such measurements were possible at the lowest two pressures in the simulations.

The numerical simulations of the SPT-140 were performed at five values of p_F as shown on Fig 2-bottom. LIF measurements were possible only for p_F=9, 15 and 30 μTorr as described in [13]. The measurements showed that the acceleration region, loosely defined here as the region within which the largest potential drop is established, remained largely unchanged at 9 and 15 μTorr. However at 30 μTorr the location at which the maximum electric field occurred was found to be ~2 mm upstream of that at 9 and 15 μTorr. In the simulations this spatial displacement was accounted for by setting the entire ν_α profile at the highest simulated pressure (30 μTorr) to be upstream of that at 9 and 15 μTorr by the same axial distance as the difference in the LIF velocity measurements.

When the simulation is of a thruster with an external cathode the boundary conditions are, in principle, three-dimensional (3-D) thus in 2-D axiymmetric simulations some assumptions must be made. In Hall2De we define a fictitious "cathode disk" around the thruster CL with inner and outer radii equal to those of the cathode boundary. Then at this boundary we reduce the true cathode ion and neutral fluxes from the cathode by the ratio of the keeper orifice area over the surface area of the cathode disk. In this manner we preserve the particle flow rates from the cathode at the expense of capturing the 3-D nature of such flows. Hence the cathode BCs are only an azimuthally-averaged representation of the true conditions during operation of a thruster with an external cathode but an accurate representation of one with a centrally mounted cathode. In the past we found the bulk plasma properties in simulations of thrusters with external cathodes to be relatively insensitive to our choice of cathode BCs because such properties are driven mostly by the magnetic field, thruster geometry, operating conditions and anomalous transport model. However, the effect of pressure on thrust is <10% and in many cases <5%; with centrally mounted cathodes the effect is even smaller [e.g. see [6, 29]]. Thus investigations of cathode BCs on thrust and any possible connections with pressure effects using 2-D axisymmetric simulations are challenging.

III. ANALYTICAL THRUST MODEL

Models of the Hall thruster performance are pervasive in the literature (e.g. see [15] and references therein). Most were derived based on semi-empirical and/or phenomenological arguments and aimed to express the total thruster efficiency, power, specific impulse, and thrust in terms of global parameters such as utilization efficiencies and operating conditions. Such models have provided valuable insight into a wide range of trends, such as the effect of the magnetic field and multiply-charged ions on performance [15]. However, the reason(s) for the observed changes in performance as a result of variations in p_F have eluded both previous phenomenological performance models as well as 2-D numerical simulations.

In this section we develop a theoretical model for the thrust that is expressed directly in terms of the principal properties of the plasma while paying special attention to contributions by the non-ionized background gas. This approach to the formulation of the model is enabled in part by the numerical simulations which provide access to all the pertinent plasma properties. The ultimate objective is to combine the thrust model with the results from the Hall2De simulations to elucidate the mechanism(s) that lead the observed thrust dependence on p_F. The approach to meet this objective is, first, to use the model to explain why the Hall2De simulations yield the near-linear trend of thrust with p_F for the range of pressures shown in Fig 2-bottom and, second, to identify process(es) that could explain the non-linear trend that is observed in the SPT-140 performance tests (Fig 2).

The total propulsive force **F** in steady state is determined by integrating the total momentum flux over a control surface S as shown by the dashed line in Fig 3

$$\mathbf{F} = \oiint_S \rho(\mathbf{u} \cdot \hat{\mathbf{n}})\mathbf{u} dA. \quad (1)$$

The total thrust T is the axial component of the force and consists of contributions from the beam ion momentum flux crossing the control surface and fast neutrals generated in the control volume υ:

$$T = T_i + T_n \quad (2)$$

where

$$T_i = \oiint_S m_i n_i (\mathbf{u}_i \cdot \hat{\mathbf{n}}) u_{i_z} dS \qquad T_n = \oiiint_\upsilon m_n \dot{n}_{cex} u_{i_z} d\upsilon. \quad (3)$$

Since we are considering only one type of heavy species (xenon) we set hereonafter $m=m_i=m_n$. The ion-neutral charge-exchange (cex) rate may be approximated as

$$\dot{n}_{cex} = n_i n_n \langle \sigma u \rangle_{cex} \approx n_i n_n \langle \sigma \rangle \langle C_{i-n} \rangle \quad (4)$$

with $\langle C_{i-n} \rangle$ denoting the average relative speed between ions and neutrals. In the Hall2De simulations the average charge-exchange collision cross section $\langle \sigma \rangle$ and $\langle C_{i-n} \rangle$ are determined using the following approximations:

$$\langle \sigma \rangle = c_{cex1} + c_{cex2} e^{-E_i^{c_3}} \qquad \langle C_{i-n} \rangle = \frac{|\mathbf{u}_i|}{\sqrt{\pi} M_i} \left[e^{-M_i^2} + \frac{\sqrt{\pi}}{2} (2M_i + M_i^{-1}) \mathrm{erf}(M_i) \right] \quad (5)$$

with the ion energy defined as $E_i \equiv m u_i^2 / 2q$ and $M_i \equiv |\mathbf{u}_i| / \sqrt{2k\Theta_i / m}$. In Eq. (5) $\langle C_{i-n} \rangle = |\mathbf{u}_i|$ when M_i>>1 (which is typically true) and $\langle \sigma \rangle$ is fixed. Hereinafter for simplicity we drop the mean symbols and express $\langle \sigma \rangle$ as σ. Also, we neglect the contributions to the thrust from all boundaries of S except the downstream boundary along which $\hat{\mathbf{n}}=\hat{z}$ and separate the two components of the ion momentum flux as follows:

$$n_i(\bar{r}) = n_{ib}^T f_i(\bar{r}) \qquad (\mathbf{u}_i \cdot \hat{\mathbf{n}}) u_{i_z}(\bar{r}) = u_{ib}^2 \cos^2\theta(\bar{r}) \quad (6)$$

where the dimensionless function f_i represents the radial variation of the ion bean density from its value at location b, n_{ib}^T, and $\bar{r} \equiv r / r_{ref}$ (see Fig 3). Then the thrust produced by the ion beam may be expressed as

$$T_i \approx m n_{ib}^T u_{ib}^2 \iint f_i \cos^2\theta dA = 2\pi m r_{ref}^2 n_{ib}^T u_{ib}^2 c_i \quad (7)$$

where

$$c_i \equiv \int f_i \cos^2\theta \bar{r} d\bar{r} \tag{8}$$

is a dimensionless factor that captures the ion beam divergence losses. We assume negligible dependence of c_i on p_F hence we determine it from the Hall2De simulations at vacuum. In Eq. (7), we have neglected the contribution of the cathode ions.

For the atomic species we define $n^F_{n_{ref}} \equiv 10\ \mu\text{Torr}/k\Theta_n$ and $\bar{n}^F_{n_{ref}} \equiv n^F_{n_{ref}}/n^T_{nb}$ where Θ_n is the temperature of the neutrals and assumed to be 500 °C. As with n^T_{ib}, the number density of propellant neutrals injected by the thruster at location b, n^T_{nb}, (see Fig 3) is determined from the Hall2De simulations at vacuum. So, we may write

$$n_n(\bar{r}) = n^T_{nb}\left[f_n(\bar{r}) + \beta \bar{n}^F_{n_{ref}}\right] \tag{9}$$

where first term in the brackets represents the radial variation of the thruster-injected neutrals along the integration boundary and the second term is the contribution from the accumulated neutrals in the facility. The linear dependence of the second term on p_F is captured by the coefficient β. Note, we have defined $\bar{n}^F_{n_{ref}}$ such that p_F=10 μTorr when β=1. The integral for the contribution of the fast neutrals then in Eq. (3) is approximated as follows

$$\oiiint_\upsilon m\dot{n}_{cex} u_{i_z} d\upsilon \approx m\ell_{cex}\sigma \iint n_i(\bar{r}) n_n(\bar{r}) u^2_{ib} \cos\theta(\bar{r}) dS. \tag{10}$$

In Eq. (10) we have estimated $d\upsilon \approx \ell_{cex} dS$ where the characteristic length ℓ_{cex} is the distance from the location where u_i=0 (see Fig 3) to point b and is approximately 9× the channel length (based on the Hall2De simulations). This implies that we neglect contributions that account for axial variations of the integrand by assuming that the ion speed instantaneously increases from 0 to its maximum value u_{ib} and that the product $n_i n_n$ does not change with z. As in Eqs. (7) and (8) the integration is over the downstream surface in Fig 3 along which $\hat{\mathbf{n}}=\hat{z}$. Then the thrust due to fast neutrals is approximately equal to

$$T_n \approx 2\pi m r^2_{ref} n^T_{ib} u^2_{ib} n^T_{nb} \sigma \ell_{cex}\left(c_{n_1} + c_{n_2}\beta \bar{n}^F_{n_{ref}}\right) \tag{11}$$

where the dimensionless coefficients c_{n_1} and c_{n_2} are given by

$$c_{n_1} = \int f_i f_n \cos\theta \bar{r} d\bar{r} \qquad c_{n_2} = \int f_i \cos\theta \bar{r} d\bar{r} \tag{12}$$

Since these coefficients involve only thruster ions and neutrals we assume they are not functions of p_F and determine them from the simulations at vacuum, as in the case of c_i (Eq. (8)).

The combination of Eqs (7) and (11) yields the total thrust

$$T \approx T_{ref}(1 - \bar{\phi}_{b/B}\bar{\phi}_{B/A})\left[c_i + n^T_{nb}\sigma\ell_{cex}\left(c_{n_1} + c_{n_2}\beta\bar{n}^F_{n_{ref}}\right)\right] \tag{13}$$

where $u_{ib}^2 \approx 2\phi_A(q/m)(1-\bar{\phi}_{b/B}\bar{\phi}_{B/A})$, $\bar{\phi}_{b/B} \equiv \phi_b/\phi_B$, $\bar{\phi}_{B/A} \equiv \phi_B/\phi_A$, and $T_{ref} = 4\pi r_{ref}^2 n_{ib}^T q\phi_A$. In this form the analytical model takes into account multiply-charged ions only through n_{ib}^T. Thus n_{ib}^T represents only an average density of all the ion species and its value is taken directly from the numerical simulations. The various plasma potentials in Eq. (13) are determined as follows. We identify the magnetic field line that begins from the intersection of the keeper exit plane and the cathode CL, location "C" on Fig 3, as our reference electron path. Along this line the electron temperature is Θ_e and the plasma potential at its intersection with the channel CL, location B in Fig 3, is given by:

$$\phi_B = \phi_C + \Theta_e \ln\left(\frac{n_{eB}}{n_{eC}}\right) \tag{14}$$

We argue that ϕ_C is largely driven by the near-cathode plasma properties and it is not affected by changes in p_F. In the thrust model calculations this property is extracted directly from the numerical simulations. Θ_e must also be determined from numerical simulations since it is driven largely by energy conservation across magnetic field lines at the channel CL. Once ϕ_C and Θ_e are known then ϕ_B relies on the electron number densities at locations B and C. To isolate the impact of the facility background we separate the total number of electrons into two main populations. The first consists of those electrons that would have existed if the thruster was operated in vacuum and the second is associated with the additional electrons produced by ionization of background atoms in the facility. The number density of the latter is defined as n_e^F. The number density of the first population can be further separated into cathode electrons, n_e^C, sometimes also termed "primary" electrons in (gridded) ion engine literature and thruster (or "secondary") electrons, n_e^T, produced by ionization of the propellant. Then at location B the electron number density is largely due to thruster electrons, n_{eB}^T:

$$n_{eB} = n_{eB}^T + n_{eB}^C + n_{eB}^F \approx n_{eB}^T \tag{15}$$

whereas at the cathode (location C), we assume the major contributions are the (primary) cathode electrons and those created by ionization of the background neutrals

$$n_{eC} = n_{eC}^T + n_{eC}^C + n_{eC}^F \approx n_{eC}^C + n_{eC}^F. \tag{16}$$

It worth noting here that for thrusters with external cathodes, n_{eC}^C may vary significantly in the azimuthal direction due to the expansion of the cathode plasma and due to the resistance imposed on the electrons by the applied magnetic field along that direction. This is therefore an inherently 3-D effect that cannot be captured by 2-D axisymmetric simulations. As mentioned in Sec. II, in Hall2De an azimuthally-averaged number density is computed, denoted here as $\tilde{n}_{eC}^C$, based on the assumption that the ion flux from the cathode boundary is reduced by the ratio of the keeper orifice opening area to the area of an annular ring that traverses 2π radians around the thruster CL. For reasons that will become evident shortly we use a factor α as follows:

$$n_{eC}^C = \alpha \tilde{n}_{eC}^C \tag{17}$$

that will allow us to assess the impact of the geometry-based azimuthal averaging by varying the effective density of these electrons. Also, for convenience we express n^F_{eC} as a function of the coefficient β as follows:

$$n^F_{eC} = \beta n^F_{eC_{ref}} \tag{18}$$

where $n^F_{eC_{ref}}$ is a reference electron number density at the cathode (location C) that is due to the background neutrals at p_F=10 μTorr. Its value is determined directly from the simulations by subtracting the computed electron number density at location C, at 9 μTorr, from the solution at vacuum and then multiplying by 10/9 to scale it to 10 μTorr (since no simulations were performed at 10 μTorr). The ratio $\bar{\phi}_{b/B}$ is determined also from the simulations. We found that for all pressures this value remained relatively unchanged at 0.8. Table 1 lists all the information that was provided by the simulations as input to the thrust model.

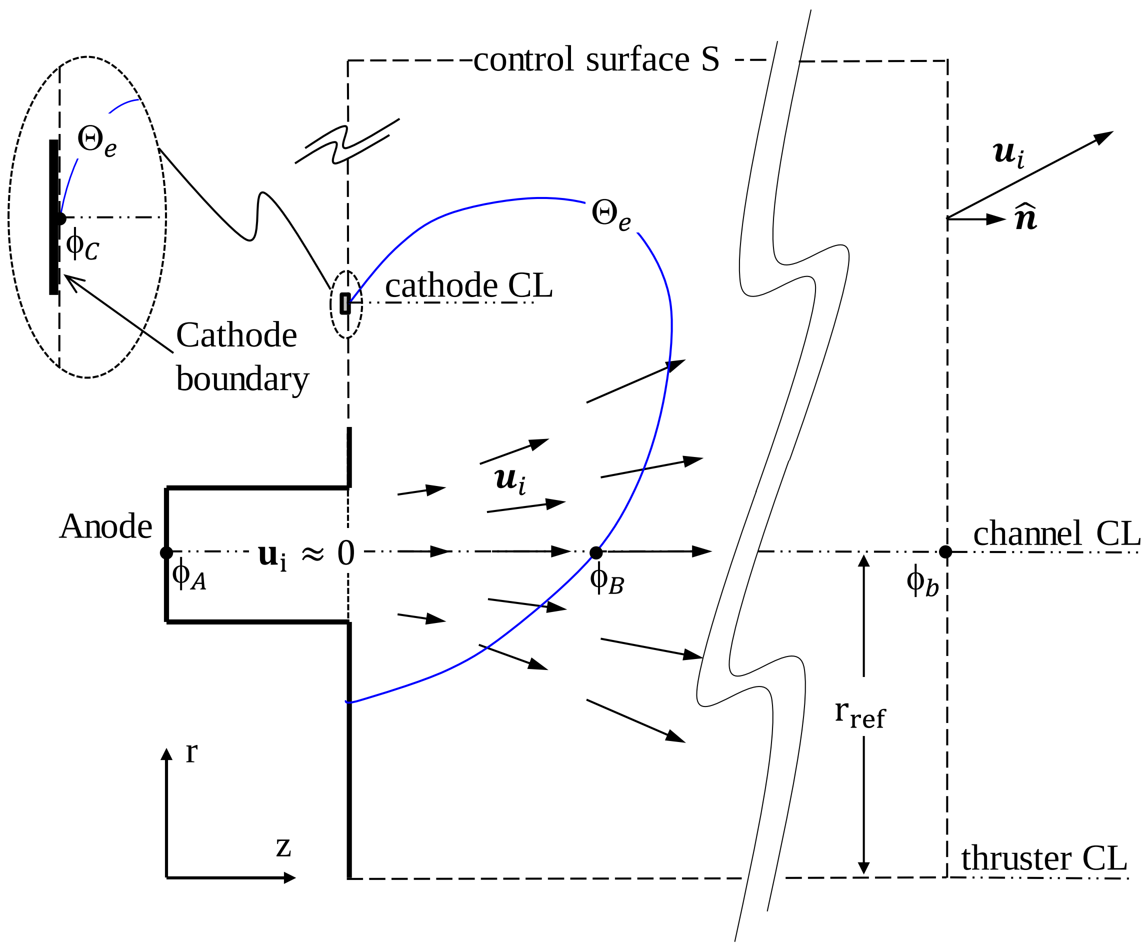

Fig 3. Schematic in reference to the theoretical model of the thrust in a Hall thruster.

Table 1. Values from the Hall2De simulations of the SPT-140 at 4.5 kW used as input in the thrust model, Eq. (13). All simulations were performed at the same discharge voltage (ϕ_A=300 V).

Property	4.5 kW
$n^F_{eC_{ref}}$ (m^{-3})	2.25×10^{15}
$\bar{\phi}_{b/B}$	0.8
Θ_e	5.5
ϕ_C	25.3
n^T_{eB}	2.7×10^{17}
$\tilde{n}^C_{eC}$	2.1×10^{15}
n^T_{nb}	1.25×10^{17}
n^T_{ib}	7.5×10^{16}
c_i	1.967
c_{n_1}	1.943
c_{n_2}	1.991

IV. MODEL RESULTS AND DISCUSSION

The comparison in Fig 2-bottom shows that the numerical simulations capture quite well the measured trend at p_F>10 μTorr but the comparison degrades at lower pressures. A closer look at the simulations reveals that for $p_F \leq 15$ μTorr the thrust variation with p_F is very close to linear and that only the solution at 30 μTorr deviates from that trend. As explained by Lopez Ortega, et al., this deviation is mainly because the acceleration region shifted upstream relative to those at p_F<30 μTorr, by about 2 mm. Such movement was evident in the LIF measurements and accounted for in the simulations through the anomalous collision frequency model as explained in Sec. II. Thus, the near asymptotic behavior of thrust at high pressures appears to be related to spatial shifts in the acceleration zone. The reason for such shifts would require a better understanding than the current state of how the anomalous electron transport is affected by the background gas and is therefore beyond the scope of this article. Here we focus on the trend at the lower pressures as it impacts directly our ability to predict in-space performance of Hall thrusters like the SPT-140.

We approach the problem in two steps. First, we employ the thrust model of Sec. III and, using the input values in Table 1, we seek to answer why the numerical solutions for $p_F \leq 15$ μTorr yield a nearly linear trend. We recall here for the reader that in these simulations no shift in the acceleration region occurred. At p_F=9 and 15 μTorr such lack of movement was confirmed by the LIF measurements; at the lower pressures for which LIF measurements were not possible, it was assumed. In the second step, we interrogate further the thrust model to identify mechanism(s) that may be responsible for the discrepancy between simulations and measurements at the lowest pressures.

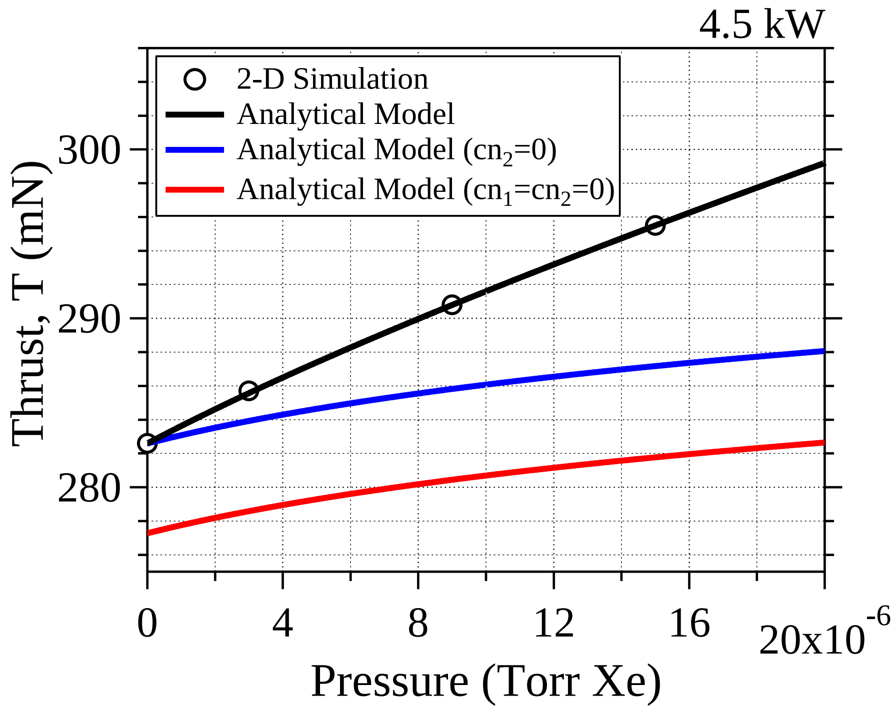

Fig 4. Comparison of the 2-D numerical simulation predictions with three different solutions of the analytical model for the thrust (Eq. (13)). For all three solutions α=1.

In Fig 4 we compare the numerical results with three different solutions from the thrust model (Eq. (13)). For all three cases it has been assumed that $n_{eC}^{C} = \tilde{n}_{eC}^{C}$ (i.e. α=1 in Eq. (17)). This means that the thrust model employed the same value for n_{eC}^{C} as the azimuthally–averaged value computed in the simulations. In the first case (cn_1=cn_2=0) the thrust contribution of all fast neutrals is neglected, that is, T_n=0 (Eq. (11)). However, referring to Eq. (14), the contribution to the cathode electrons (and, in turn, to the plasma potential) associated with the background neutrals (n_{eC}^{F}) is taken into account. The analytical solution yields a linear rise of the thrust with p_F but at a smaller slope than that in the simulations. Also, the thrust values for all pressures are lower than those from the simulations. This under-estimation quantifies the significance of the fast neutrals to the thrust but also reveals a more subtle finding: the thrust rises with p_F, even in the absence of fast neutrals. We found this is because the additional electrons produced by the ionization of the background neutrals lowers the plume potential, ϕ_B, as determined by Eq. (14). This effect is therefore associated with the transport of electrons *along* magnetic field lines, not perpendicular to them. As expected, since n_{eC}^{F} is the only remaining link to background neutrals we find that the thrust remains invariant with p_F when n_{eC}^{F}=0.

In the second analytical solution on Fig 4 (cn_2=0), we account for fast neutrals produced by charge-exchange between the ion beam and the thruster neutrals ($cn_1 \neq 0$) but exclude those produced due to the background gas (cn_2=0). As expected, the theoretical model predicts the thrust in the simulation at vacuum but continues to under-predict the slope of thrust vs. p_F. It is only with the third analytical solution (cn_1,$cn_2 \neq 0$), which adds also the background neutrals in Eq. (13), we achieve excellent agreement with the simulation results. Hence, the three cases clearly distinguish how the background gas influences the computed thrust in the numerical simulations. The results also suggest that the thrust model captures well the mechanisms that drive the numerical solution. But since neither capture the measured trend at low pressures it also implies that the mechanism(s) that drive this trend is/are remain elusive. Below, we propose one such mechanism.

For reason that will become evident shortly, we re-write Eq. (14) in a form that includes explicitly the particle densities of the various electron populations

$$\phi_B = \phi_C + \Theta_e \ln\left(\frac{n_{eB}^T}{\alpha\tilde{n}_{eC}^C + \beta n_{eC_{ref}}^F}\right) \quad (19)$$

and note from Table 1 that when $\alpha = \beta = 1$, $\alpha\tilde{n}_{eC}^C$ is comparable to $\beta n_{eC_{ref}}^F$. This means that for large values of β (i.e. large p_F) the second term in the denominator dominates but as $\beta \rightarrow 0$ the first term dominates. Thus, for large β the contribution to the thrust through changes in the plume plasma potential (ϕ_B) is reduced and the thrust is largely driven by the production rate of fast neutrals. Since this is proportional to the background gas density the thrust variation with p_F becomes increasingly linear when no spatial displacement of the acceleration zone occurs. This is indeed what is observed in the simulations [13]. On the other hand as $\beta \rightarrow 0$ the cathode electrons ($\alpha\tilde{n}_{eC}^C$) drive the change in thrust through the plume plasma potential ϕ_B as the contribution from fast neutrals diminishes. Because the dependence of ϕ_B on the electron particle densities is logarithmic the thrust variation with β (and thus p_F) would then be non-linear. However, in the solution of Fig 4 with α=1 and $cn_1, cn_2 \neq 0$ we find that $\tilde{n}_{eC}^C$ is too high relative to $\beta n_{eC_{ref}}^F$ to allow the second to dominate over the first in Eq. (19) as β decreases. Thus, the trend in this solution at low pressures does not deviate much from linearity and the thrust at $\beta = 0$ is determined simply by the ratio $n_{eB}^T/\tilde{n}_{eC}^C$.

As described in Sec. II, in the 2-D simulations $\tilde{n}_{eC}^C$ is determined by averaging the plasma flux at the cathode boundary over a disk of radius that is comparable to the distance of the external cathode from the thruster CL. Thus, $\tilde{n}_{eC}^C$ represents only an azimuthally-averaged value of the true cathode electron density. In reality however such geometric averaging may be far from representative of the effective density around the thruster since in the azimuthal direction the cathode electrons expand rapidly while their motion in this direction is inhibited by the applied magnetic field. In fact the rapid decrease of the density in this direction can be inferred from visual inspection of the plasma near the cathode in Fig 1-left where a highly collimated cathode plume is clearly evident. Our hypothesis then is twofold. First, the main coupling between cathode and thruster occurs largely through this collimated region (reference magnetic field line in Fig 3). Second, the relatively small perturbations in the thrust that show strong coupling to the facility pressure are related to the details of how the electron flow from the cathode is azimuthally distributed around the thruster. If true this would imply that the actual value of the thrust in vacuum is determined mainly by the ratio $n_{eB}^T/\tilde{n}_{eC}^C$ and that the larger the asymmetry the lower the $\tilde{n}_{eC}^C$ and, consequently, the larger the sensitivity of thrust to p_F. This would explain the results of Hofer, et al., who found that thrust sensitivity to p_F decreased as an external cathode in a 6-kW laboratory Hall thruster was moved closer to the acceleration channel [6]. Naturally, the limiting case of such an experiment is a centrally mounted cathode which indeed has been shown to exhibit the least sensitivity since the cathode flow is exactly azimuthally symmetric (e.g. see [6, 29]). Thus, it is important to recognize here that the significance of the parallel transport (Eq (14)) on the pressure-dependent thrust perturbations relies also on the details of the applied magnetic field topology in the vicinity of the external cathode. If for example, the magnetic field lines form a separatrix in this region and the location of the cathode relative to it makes it difficult for electrons to cross these lines, then this is an effect in the r-z plane in which perpendicular transport can play a more dominant role than parallel transport.

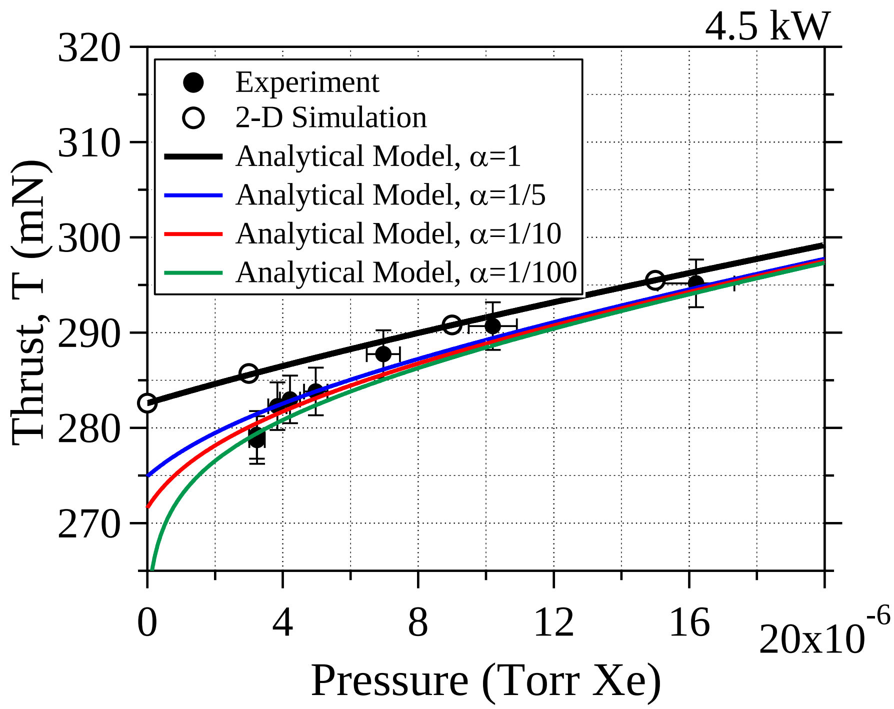

Fig 5. Comparison between Hall2De simulations, measurements and solutions of the analytical; thrust model (Eq. (13)) for different values of the coefficient α.

Clearly azimuthal variations of the cathode plasma is an inherently 3-D problem and therefore outside the capability of a r-z axisymmetric simulation. However, we can assess the hypothesis using the thrust model. In Fig 5 we plot solutions of Eq. (13) for $\alpha<1$ and compare them with the original solution $\alpha=1$ as well with the measured thrust. In doing so we are using α as a means to account for azimuthal asymmetries on the effective density of cathode electrons $\alpha\tilde{n}_{eC}^{C}$. The comparison with $\alpha<1$ shows excellent agreement with the measured thrust at the higher pressures and, as expected, reduced dependence on α since with increasing β, $\beta n_{eC_{ref}}^{F}$ and the fast neutrals dominate the contributions to the thrust. At low β (i.e. low p_F) however deviations from linearity become larger as α is lowered and the measured behavior is predicted more closely by the thrust model. This improved comparison suggests that in the absence of spatial displacements of the acceleration region, azimuthal asymmetries in the cathode flow could indeed be driving the thrust sensitivity at the lowest facility pressures. It also underscores the need for 3-D simulations of Hall thrusters with external cathodes and/or plasma measurements in the azimuthal direction that are focused on better quantifying the true value of α.

V. CONCLUSIONS

Psyche will be the first mission to use (SPT-140) Hall thrusters beyond lunar orbit. Performance tests of the SPT-140 in VF-5 at NASA GRC produced the now well-observed but poorly understood dependence of thrust on backpressure. The observed thrust variation over a ~10× change in backpressure was highest at the highest discharge power (4.5 kW), and was larger than that observed in tests of the SPT-100 over approximately the same backpressure range. Since the true near-vacuum conditions in space cannot be reproduced even in our best vacuum facilities when a Hall thruster is operating, such degradation in thrust yields large uncertainties in spaceflight performance predictions. Recent mission design work for Psyche has led to a greater understanding and appreciation of the impact of precisely these uncertainties on mission performance. It has been found that larger uncertainties could drive propellant and power margin allocations to both double. Moreover, the required conservatism for trajectory analysis can lead to reductions in delivered mass by several tens of kilograms and longer trip times, driving up operations costs.

2-D (r-z) axisymmetric simulations of the SPT-140 were performed with the Hall2De code to reduce the uncertainty in space flight predictions. The simulations aimed, first, to validate the numerical results using measurements from the performance tests and, second, to provide estimates of thruster life for the Psyche throttle profile. The simulations captured well the measured thrust at pressures $\gtrsim$10 μTorr but the comparison degraded at lower pressures. In our companion paper Lopez Ortega, et al, performed sensitivity simulations in which the acceleration region at pressures < 9 μTorr was shifted downstream of the anode by less than a couple of millimeters. We found that such shifts were sufficient to capture the observed thrust trend thereby offering a possible explanation for the original discrepancy in the simulations. We also recognized however that at the intermediate pressures, LIF measurements revealed no spatial shifts of the acceleration region when the pressure was reduced from 15 to 9 μTorr. No LIF measurements were possible at values < 9 μTorr. Thus, though such shifts at low pressures are possible the physics that would drive them are not known.

An analytical model of the thrust has been developed and applied in this article to further elucidate the observed trends in the simulations first and, ultimately, in the measurements. Inputs to the model were provided by the Hall2De simulations. The combined analyses reveals that thrust rise with pressure is very close to linear in the simulations largely due to two contributions: (1) fast neutrals produced by charge-exchange collisions between beam ions and the background atoms and, (2) enhanced ion acceleration by a decrease of the near-plume potential, caused by the additional electrons generated due to the presence of the background gas. The first is a purely linear effect as it depends directly on the background neutral gas density. The second is dependent on the transport of electrons along magnetic field lines that link the thruster plume to the cathode and is, in principle, a non-linear effect since it depends on Boltzmann's law for the electrons. However, in the simulations because the azimuthally-averaged density of cathode electrons is high the non-linearity was found to be weak.

The azimuthally-averaged density in the simulations is estimated based on geometric area ratio arguments. However, the above-mentioned findings led to the recognition that the distribution of electrons from an external cathode can be highly asymmetric in the azimuthal direction because their expansion occurs in the presence of an applied magnetic field that impedes their motion in this direction. Indeed, visual inspection of the near-plume during on-ground operation of the SPT-140 shows clearly that the cathode discharge is highly collimated. Therefore, geometric averaging can grossly over-estimate the effective density of these electrons. Since this is an inherently 3-D effect 2-D (r-z) simulations would not be able to capture it. However, using the thrust model we performed a series of sensitivity calculations in which we decreased the azimuthally-average density of cathode electrons by 5-100 times and showed excellent agreement with the non-linear thrust trend measured at the lowest pressures. Due to the logarithmic dependence of the plume potential on the electron densities, these calculations show that the true value of thrust in vacuum is strongly dependent on the details of the distribution of primary electrons from the cathode around the thruster. As the facility pressure increases secondary electrons generated by ionization of the background gas overshadow the azimuthal variabilities of the primary electrons and drive the thrust back to a linear dependence on pressure. This linearity is broken again as the pressure increases further due to movement of the acceleration region.

The above hypothesis would explain the findings of previous tests with a different Hall thruster in which the location of the external cathode was varied. It was found in those tests that thrust dependence on pressure decreased as the cathode was moved closer to the acceleration channel. By extension, the hypothesis would also explain the insensitivity of performance in thrusters with centrally mounted cathodes as well as the longstanding challenges 2-D axisymmetric simulations have had in uncovering the source behind these pressure effects. Most critically for the SPT-140 however, and the Psyche mission by extension, the findings suggest that the uncertainly in the thrust predictions during spaceflight can be reduced significantly by a combination of modeling and measurements that take into account pertinent variations in the azimuthal direction.

ACKNOWLEDGMENTS

The research described in this paper was carried out by the Jet Propulsion Laboratory, California Institute of Technology, under a contract with the National Aeronautics and Space Administration. Reference herein to any specific commercial product, process, or service by trade name, trademark, manufacturer, or otherwise, does not constitute or imply its endorsement by the United States Government or the Jet Propulsion Laboratory, California Institute of Technology. The authors would like to thank NASA's Planetary Science Division, NASA's Discovery Program Office, and JPL's Solar System Exploration Directorate for their support of this work.

REFERENCES

[1] D. Y. Oh, S. Collins, D. M. Goebel, B. Hart, G. Lantoine, J. S. Snyder, G. Whiffen, L. Elkins-Tanton, P. Lord, Z. Pi, and L. Rotlisburger, "Development of the Psyche Mission for NASA's Discovery Program," in 35th International Electric Propulsion Conference, Atlanta, GA, USA, IEPC-2017-153, October 2017.

[2] J. S. Snyder, D. M. Goebel, V. H. Chaplin, A. Lopez Ortega, I. G. Mikellides, F. Aghazadeh, I. Johnson, T. Kerl, and G. Lenguito, "Electric Propulsion for the Psyche Mission," in 36th International Electric Propulsion Conference, Vienna, Austria, IEPC-2019-244, September 2019.

[3] J. S. Snyder, G. Lenguito, J. D. Frieman, T. Haag, and J. A. Mackey, "The Effects of Background Pressure on SPT-140 Hall Thruster Performance," in 2018 Joint Propulsion Conference, Cincinnati, OH, AIAA-2018-4421, July 2018, pp. 4421.

[4] K. D. Diamant, R. Liang, and R. L. Corey, "The Effect of Background Pressure on SPT-100 Hall Thruster Performance," in 50th AIAA/ASME/SAE/ASEE Joint Propulsion Conference, Cleveland, OH, AIAA-2014-3710, July 2014, pp. 3710.

[5] H. Kamhawi, W. Huang, T. Haag, and R. Spektor, "Investigation of the Effects of Facility Background Pressure on the Performance and Operation of the High Voltage Hall Accelerator," in 50th AIAA/ASME/SAE/ASEE Joint Propulsion Conference, Cleveland, OH, AIAA-2014-3707, July 2014, pp. 3707.

[6] R. R. Hofer, and J. R. Anderson, "Finite Pressure Effects in Magnetically Shielded Hall Thrusters," in 50th AIAA/ASME/SAE/ASEE Joint Propulsion Conference, Cleveland, OH, AIAA-2014-3709, July 2014, pp. 3709.

[7] D. Byers, and J. W. Dankanich, "A Review of Facility Effects on Hall Effect Thrusters," in 31st International Electric Propulsion Conference, Ann Arbor, MI, USA, IEPC 2009-076, September 2009.

[8] M. L. R. Walker, A. L. Victor, R. R. Hofer, and A. D. Gallimore, "Effect of backpressure on ion current density measurements in hall thruster plumes," *Journal of Propulsion and Power*, vol. 21, no. 3, pp. 408-415, May-Jun, 2005.

[9] D. L. Brown, and A. D. Gallimore, "Evaluation of Facility Effects on Ion Migration in a Hall Thruster Plume," *Journal of Propulsion and Power*, vol. 27, no. 3, pp. 573-585, May-Jun, 2011.

[10] M. R. Nakles, and W. A. Hargus, "Background Pressure Effects on Ion Velocity Distribution Within a Medium-Power Hall Thruster," *Journal of Propulsion and Power*, vol. 27, no. 4, pp. 737-743, Jul-Aug, 2011.

[11] J. D. Frieman, S. T. King, M. L. R. Walker, V. Khayms, and D. King, "Role of a Conducting Vacuum Chamber in the Hall Effect Thruster Electrical Circuit," *Journal of Propulsion and Power*, vol. 30, no. 6, pp. 1471-1479, Nov-Dec, 2014.

[12] J. A. Walker, J. D. Frieman, M. L. R. Walker, V. Khayms, D. King, and P. Y. Peterson, "Electrical Facility Effects on Hall-Effect-Thruster Cathode Coupling: Discharge Oscillations and Facility Coupling," *Journal of Propulsion and Power*, vol. 32, no. 4, pp. 844-855, Jul, 2016.

[13] A. Lopez Ortega, I. G. Mikellides, V. H. Chaplin, D. Snyder, and G. Lenguito, "SPT-140 TBD," *Plasma Sources Science & Technology*, vol. XX, no. X, Under Review, 2019.

[14] I. G. Mikellides, and I. Katz, "Numerical simulations of Hall-effect plasma accelerators on a magnetic-field-aligned mesh," *Physical Review E*, vol. 86, no. 4, pp. 046703, Oct 17, 2012.

[15] R. R. Hofer, *Development and characterization of high-efficiency, high-specific impulse xenon Hall thrusters*, 2004.

[16] D. M. Goebel, and I. Katz, *Fundamentals of electric propulsion : ion and Hall thrusters*, Hoboken, N.J.: Wiley, 2008.

[17] I. G. Mikellides, I. Katz, and R. R. Hofer, "Design of a Laboratory Hall Thruster with Magnetically Shielded Channel Walls, Phase I: Numerical Simulations," in 47th AIAA/ASME/SAE/ASEE Joint Propulsion Conference, San Diego, CA, AIAA-2011-5809, July 2011, pp. 5809.

[18] I. G. Mikellides, I. Katz, R. R. Hofer, and D. M. Goebel, "Design of a Laboratory Hall Thruster with Magnetically Shielded Channel Walls, Phase III: Comparison of Theory with Experiment," in 48th AIAA/ASME/SAE/ASEE Joint Propulsion Conference, Atlanta, GA, AIAA-2012-3789, July 2012.

[19] A. Lopez Ortega, and I. G. Mikellides, “A New Cell-Centered Implicit Numerical Scheme for Ions in the 2-D Axisymmetric Code Hall2De,” in 50th AIAA/ASME/SAE/ASEE Joint Propulsion Conference, Cleveland, OH, AIAA-2014-3621, July 2014.

[20] S. I. Braginskii, "Transport Processes in a Plasma," *Reviews of Plasma Physics,* M. A. Leontovich, ed., pp. 205-311, New York: Consultants Bureau, 1965.

[21] I. Katz, and I. G. Mikellides, “Neutral gas free molecular flow algorithm including ionization and walls for use in plasma simulations,” *Journal of Computational Physics,* vol. 230, no. 4, pp. 1454-1464, Feb 20, 2011.

[22] A. Lopez Ortega, and I. G. Mikellides, “The Importance of the Cathode Plume and its Interactions with the Ion Beam in Numerical Simulations of Hall thrusters,” in 34th International Electric Propulsion Conference, Hyogo-Kobe, Japan, IEPC-2015-310, July 2015.

[23] J. C. Adam, A. Heron, and G. Laval, “Study of stationary plasma thrusters using two-dimensional fully kinetic simulations,” *Physics of Plasmas,* vol. 11, no. 1, pp. 295-305, Jan, 2004.

[24] A. Ducrocq, J. C. Adam, A. Heron, and G. Laval, “High-frequency electron drift instability in the cross-field configuration of Hall thrusters,” *Physics of Plasmas,* vol. 13, no. 10, Oct, 2006.

[25] S. Tsikata, N. Lemoine, V. Pisarev, and D. M. Gresillon, “Dispersion relations of electron density fluctuations in a Hall thruster plasma, observed by collective light scattering,” *Physics of Plasmas,* vol. 16, no. 3, Mar, 2009.

[26] J. Cavalier, N. Lemoine, G. Bonhomme, S. Tsikata, C. Honore, and D. Gresillon, “Hall thruster plasma fluctuations identified as the E x B electron drift instability: Modeling and fitting on experimental data,” *Physics of Plasmas,* vol. 20, no. 8, Aug, 2013.

[27] P. Coche, and L. Garrigues, “A two-dimensional (azimuthal-axial) particle-in-cell model of a Hall thruster,” *Physics of Plasmas,* vol. 21, no. 2, Feb, 2014.

[28] I. G. Mikellides, and A. L. Ortega, “Challenges in the development and verification of first-principles models in Hall-effect thruster simulations that are based on anomalous resistivity and generalized Ohm's law,” *Plasma Sources Science & Technology,* vol. 28, no. 1, Jan, 2019.

[29] H. Kamhawi, W. Huang, T. Haag, R. Shasrty, R. Thomas, J. Yim, D. A. Herman, G. Williams, J. Myers, R. R. Hofer, I. G. Mikellides, M. J. Sekerak, and J. E. Polk, “Performance and Facility Background Pressure Characterization Tests of NASAs 12.5-kW Hall Effect Rocket with Magnetic Shielding Thruster,” in 34th International Electric Propulsion Conference, Hyogo-Kobe, Japan, IEPC-2015-007, July 2015.